Transitions between imperfectly ordered crystalline structures: A phase switch Monte Carlo study

Dorothea Wilms,[1] Nigel B. Wilding,[2] and Kurt Binder[1]
[1]*Institut für Physik, Johannes Gutenberg Universität Mainz, Staudinger Weg 7, 55099 Mainz, Germany*
[2]*Department of Physics, University of Bath, Bath BA2 7AY, United Kingdom*
(Received 7 March 2012; published 18 May 2012)

A model for two-dimensional colloids confined laterally by "structured boundaries" (i.e., ones that impose a periodicity along the slit) is studied by Monte Carlo simulations. When the distance D between the confining walls is reduced at constant particle number from an initial value D_0, for which a crystalline structure commensurate with the imposed periodicity fits, to smaller values, a succession of phase transitions to imperfectly ordered structures occur. These structures have a reduced number of rows parallel to the boundaries (from n to $n-1$ to $n-2$, etc.) and are accompanied by an almost periodic strain pattern, due to "soliton staircases" along the boundaries. Since standard simulation studies of such transitions are hampered by huge hysteresis effects, we apply the phase switch Monte Carlo method to estimate the free energy difference between the structures as a function of the misfit between D and D_0, thereby locating where the transitions occur in equilibrium. For comparison, we also obtain this free energy difference from a thermodynamic integration method: The results agree, but the effort required to obtain the same accuracy as provided by phase switch Monte Carlo would be at least three orders of magnitude larger. We also show for a situation where several "candidate structures" exist for a phase, that phase switch Monte Carlo can clearly distinguish the metastable structures from the stable one. Finally, applying the method in the conjugate statistical ensemble (where the normal pressure conjugate to D is taken as an independent control variable), we show that the standard equivalence between the conjugate ensembles of statistical mechanics is violated.

DOI: 10.1103/PhysRevE.85.056703 PACS number(s): 02.70.Tt, 64.75.Xc, 05.70.Fh, 64.60.an

I. INTRODUCTION

Periodically ordered arrays of nanoparticles, colloidal crystals, crystalline mesophases formed from surfactant molecules or block copolymers, etc., are all examples of complex periodic structures that can occur in soft matter systems. Since often the interactions between the constituent particles of these structures are to a large degree tunable, one has the possibility of producing materials with "tailored" properties which have potential applications in nanotechnological devices [1–5]. When seeking to provide theoretical guidance for understanding structure-property relations in such complex soft matter systems, a basic issue is how to judge the relative stability of competing candidate structures, that is, to distinguish the stable structure (having the lowest free energy) from the metastable ones. For standard crystals formed from atoms or small molecules, this question can be answered by comparing ground state energies of the competing structures (and, if necessary, also taking entropic contributions from lattice vibrations into account, within the framework of the harmonic approximation). In soft matter systems, disorder in the structure and thermally driven entropic effects rule out such an approach, and hence there is a need for computer simulation methods that compute the free energy of the various complex structures. However, as is well known, the free energy of a model system is not a direct output of either molecular dynamics or Monte Carlo simulations, and special techniques have to be used [6–11].

In principle, one can obtain the absolute free energy of a structure by linking it to some reference state of known free energy by means of thermodynamic integration (TI) [6–16]. The strengths of TI are that it is both conceptually simple and often straightforward to implement. Its principal drawback is that the quantity of interest, namely the free energy *difference* between candidate structures, is typically orders of magnitude smaller than the absolute free energies of the individual structures which TI measures. Essentially, therefore, TI estimates a small number by taking the difference of two large ones; as a consequence, the precision of the method is limited and an enormous (even sometimes wasteful) investment of computer resources may be needed to resolve the free energy difference accurately [9].

A much more elegant approach, albeit one which is not quite so easy to implement as TI, is the "phase switch Monte Carlo" [17–23] technique. This method is potentially more powerful than TI because it focuses directly on the small free energy difference between the structures to be compared, rather than their absolute free energies. In previous work, the precision of the method was demonstrated in the context of measurements of the free energy difference between fcc and hcp structures of hard spheres [17,19] and the phase behavior of Lennard-Jones crystals [20] and as a means of studying liquid-solid phase transitions [18]. In the latter case, simple model systems containing only a few hundred particles could be studied, while for the study of the fcc-hcp free energy difference [17,21] larger systems of up to 1728 particles could be studied by virtue of the fact that these crystals differ only in their packing sequence of close-packed triangular defect-free lattice planes. However, it is an open question what system sizes one can attain with the phase switch method for more general crystalline systems, including—as in the present work—ones which exhibit considerable structural disorder ("soliton staircases," see below). Furthermore, there have hitherto been no like-for-like comparisons of the TI method and the phase switch method on the same system, so while there are good reasons for *presuming* the superiority of phase switch (in terms of precision delivered for a given computational investment), this has never actually been quantified.

In the present paper, we address these matters, considering as a generic example a two-dimensional colloidal crystal in varying geometrical confinement [24–28]. As is well known, two-dimensional colloidal crystals are experimentally much studied model systems [29–40] comprising, for example, polystyrene spheres containing a superparamagnetic core adsorbed at the air-water interface. Applying a magnetic field oriented perpendicular to this interface creates a repulsive interaction that scales like r^{-3} (r being the particle separation), whose magnitude is controlled by the magnetic field strength [29]. Lateral confinement of such two-dimensional crystals can be effected mechanically or by laser fields (if the latter are also applied in the bulk of such a crystal, one can study laser-induced melting and/or freezing [41–44]). Of course, there exist many related problems in rather different physical contexts ("dusty plasmas" [45,46], i.e., negatively charged SiO_2 fine particles with 10 μm diameter in weakly ionized rf discharges; lattices of confined spherical block copolymer micelles [47]; vortex matter in slit channels [48], etc.). However, our study does not address a specific system; rather we focus on the methodological aspects of how one can study such problems by computer simulation.

The outline of the present paper is a follows. In Sec. II, we summarize the key facts about our model, namely strips of two-dimensional crystals confined between two walls where structural phase transitions may occur when the distance between the (corrugated) rigid boundaries is varied [25–28,49–51] (i.e., a succession of transitions in the number of crystal rows n parallel to the walls occur, $n \to n-1 \to n-2$, with increasing compression, accompanied by the formation of a "soliton staircase" at the walls [25–28]). In Sec. III, the methods that are used are briefly described: The TI method of Schmid and Schilling [15,16] is used as a baseline, while the main emphasis is on the phase switch Monte Carlo method (implementation details of which are deferred to the Appendix). In Sec. IV we describe the results of the application of these techniques to the model of Sec. II. We show that phase switch Monte Carlo [18–20] can accurately locate the phase transitions, despite the need to deal with thousands of particles, and is orders of magnitude more efficient than TI. Section V summarizes some conclusions.

II. STRUCTURAL TRANSITIONS IN CRYSTALLINE STRIPS CONFINED BY CORRUGATED BOUNDARIES: PHENOMENOLOGY

Here we introduce the model for which our methodology is exemplified and recall briefly the main findings concerning the rather unconventional transitions that have been detected [25–28], as far as they are relevant for the present study.

We consider monodisperse colloidal particles in a strictly two-dimensional geometry, which then are treated like point particles in a plane interacting with a suitable effective potential $V(r)$ that depends only on the interparticle distance r. In the real systems [29,31–35] this potential is purely repulsive, but due to the magnetostatic dipole-dipole interaction (whose strength is controlled by the external magnetic field) it is very slowly decaying, $V(r) \propto r^{-3}$. Since we here are not concerned with quantitative comparisons with real experimental data on such systems, we simplify the problem by adopting a computationally more efficient r^{-12} potential, in accord with previous work [25–28]. Moreover, to render it strictly short-ranged, we introduce a cutoff r_c, such that $V(r \geqslant r_c) \equiv 0$, and employ a smoothing function to make $V(r)$ differentiable at $r = r_c$. Thus, the model potential used is

$$V(r) = \varepsilon[(\sigma/r)^{12} - (\sigma/r_c)^{12}]\left[\frac{(r-r_c)^4}{h^4 + (r-r_c)^4}\right], \qquad (1)$$

with parameters $r_c = 2.5\sigma$ and $h = 0.01\sigma$. Henceforth, the particle diameter $\sigma = 1$ defines the length units in our model, and for the energy scale, $\varepsilon = 1$ is taken, while Boltzmann's constant $k_B = 1$. It is known that at $T = 0$ the ground state of this model is a perfect triangular lattice, with a lattice spacing a related to the choice of the number density $\rho = N/V$ [with N the particle number and V the (two-dimensional) "volume" of the system] via

$$a^2 = 2/(\sqrt{3}\rho). \qquad (2)$$

Assuming the physical effect of truncating the potential can be neglected, only the choice of the combination $X = \rho(\varepsilon/k_B T)^{1/6}$ controls the phase behavior [52]. Thus, following previous work in the NVT ensemble it suffices to choose a single density when the temperature variation is considered [25,53]. For the particular choice $\rho = 1.05$, the melting transition of this model is known to occur at about $T = T_m \approx 1.35$ [53]. Note that here we are not at all concerned with the peculiarities of melting in two dimensions [54], and hence we focus on a temperature deep within the crystalline phase, $T = 1$. Although it is known that the density of vacancies and interstitials in $d = 2$ for any nonzero temperature is also nonzero in thermal equilibrium [54,55], for the chosen particle number $N = 3240$ the system is essentially defect free, since the densities of these point defects at $T = 1$ are extremely small [25,53].

The geometry of the present system is a $D \times L_x$ slit, confined in the y direction and periodic in the x direction. In the y direction there are $n_y = 30$ rows of the triangular lattice, each containing $n_x = 108$ particles, stacked upon each other. The x direction coincides with a lattice direction so that $L_x = n_x a$. The confining boundaries (one at the top and one at the bottom of the system) each take the form of a double row of particles in which the particles are rigidly fixed at the sites of a perfect triangular lattice (Fig. 1). These rows of fixed particles represent rigid corrugated walls, essentially acting as a periodic wall potential on the mobile particles. The mobile particles cannot slip between the wall particles. The second row of wall particles is necessary, though, as the range of the potential is large enough for the particles in the first row of mobile particles to feel the potential exerted by the particles in both rows of the wall. A single row of wall particles would therefore not create the correct potential for this crystalline structure.

While the distance of the first row at the upper wall from the first row of mobile particles in the ideal stress-free crystal is simply $D = n_y a\sqrt{3}/2$, in the following we are interested in the response of the system when the walls occur at a smaller distance, caused by a misfit Δ, defined via [56]

$$D = (n_y - \Delta)a\sqrt{3}/2. \qquad (3)$$

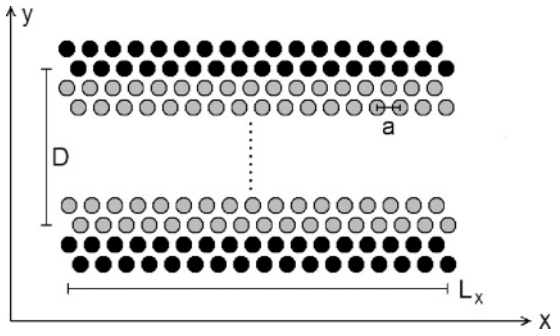

FIG. 1. Sketch of the system geometry, showing the fixed wall particles (black circles) and the mobile particles (gray circles). The orientation of the coordinate axes is indicated, as well as the lattice spacing of the triangular lattice (a) and the linear dimensions L_x, D of the system.

As described in the previous work [25–28], standard Monte Carlo simulation [6,7] allows one to study this model at various values of Δ, and also sample the stress $\sigma = \sigma_{yy} - \sigma_{xx}$ ($\sigma_{\alpha\beta}$ are the Cartesian components of the pressure tensor) applying the virial formula [6,7]. Figure 2 shows that when one starts out with the perfect crystal ($n_y = 30$) with no misfit, the crystal already shows a small finite stress, because the rigid wall particles somewhat hinder the vibrations of the mobile particles in their potential wells, but this effect is of no importance here. Rather we focus on the (slightly nonlinear) increase of the stress up to about $\Delta = \Delta_c \approx 2$, followed by the (almost) discontinuous decrease, and the subsequent increases again with further enhancement of the misfit. A previous structural analysis has revealed [25–28] that the sudden decrease of stress is due to a transition in the number of rows in the crystal, $n_y \to n_y - 1 = 29$. However, since in the *NVT* ensemble the particle number is conserved, the $n_x = 108$ particles of the row that disappears must be redistributed among the remaining rows. A closer examination of the structure revealed that none of these particles enter the two rows adjacent to the rigid walls; instead they all go into the $n_y - 3 = 27$ rows of the system that are further

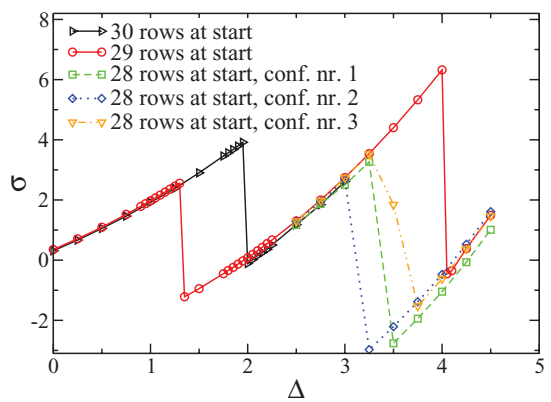

FIG. 2. (Color online) Stress σ plotted vs misfit Δ for a system of $N = 3240$ particles and using different starting configurations having $n_y = 30$, $n_y = 29$, and $n_y = 28$, as indicated in the figure. Note the huge hysteresis of the $n_y = 30 \to n_y = 29$ and $n_y = 29 \to n_y = 28$ transitions. For further explanations, see main text.

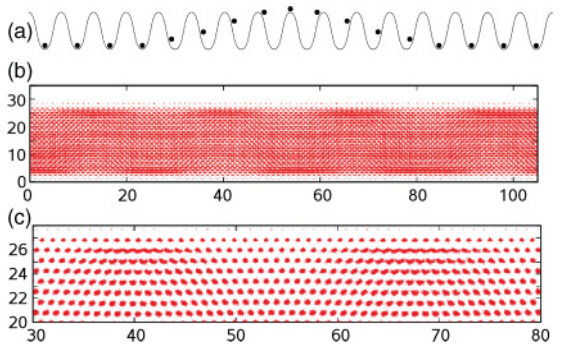

FIG. 3. (Color online) (a) Putting $n + 1$ particles in a periodic potential with n minima creates a soliton configuration, that is, over a range of several lattice spacings particles are displaced from the potential minima (schematic). (b) Superimposed snapshot pictures of 750 configurations of the particle positions, where for a system of $n_y = 30$ rows and a large misfit ($\Delta = 2.6$) a transition to $n_y - 1 = 29$ rows has occurred ($n_x = 108$ and $T = 1.0$ were chosen). The four solitons at each wall are visible due to the larger lateral displacements of the particles, leading to a darker region in the snapshot. Panel (c) shows a close-up of the structure near the upper wall. Numbers shown along the axes indicate the Cartesian coordinates of the particles. Panels (b) and (c) have been adapted from Chui *et al.* [25].

away from the walls. Thus, in the present case, the particle number per row becomes $n_x' + n_x/(n_y - 3) = n_x + 4$, and this leads to a new lattice spacing in the x direction of $a' = a/(1 + 4/n_x)$, which is no longer commensurate with the spacing between the particles forming the rigid walls (or the two immediately adjacent layers which remain commensurate with them). While for the rows in the center of the system (near $n_y/2$) this compression of the lattice spacing occurs uniformly along the x direction, this is not the case close to the walls, which provide a periodic potential (with periodicity a) that acts on the row of mobile particles a little further inside the slit. The fact that on the scale L_x the effective wall potential exhibits n_x minima but $n_x' = n_x + 4$ particles need to be accommodated leads to the formation of a lattice of solitons close to both walls ("soliton staircase") [57,58], as depicted for an idealized case in Fig. 3.

In practice, the actual structure having $n_y - 1 = 29$ rows that is formed in the simulations on increasing the misfit Δ beyond the critical value Δ_c, is generally less regular than the "idealized" one shown in Fig. 3: Specifically, the relative distance between neighboring solitons showed a considerable variation. This comes about because (i) the solitons are formed from the stressed crystal with $n_y = 30$ rows via random defect nucleation events [26] and (ii) the mutual interaction between neighboring solitons, which is the thermodynamic driving force toward a regular soliton arrangement, is very small [27]. Despite this, it is nevertheless reasonable to construct "by hand" the expected regular structure of $n_x/(n_y - 3)\,(= 4)$ solitons near each wall as a starting configuration for a system with 29 rows, which can subsequently be equilibrated [25]. Of course, there is no guarantee that this guessed structure actually is the one lowest in free energy; but it does exhibit slightly less stress than all other structures that had been tested, for misfits in the range $1.5 \leqslant \Delta \leqslant 3$, and hence has been used

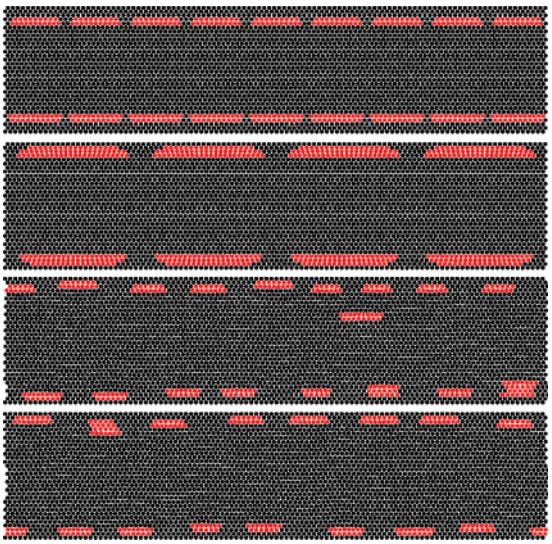

FIG. 4. (Color online) Configurations with $N = 3240$ particles and $n_y - 2 = 28$ rows, but different configurations of the solitons. In the text, they are referenced as "configuration numbers 1, 2, 3, and 4" from top to bottom. For a clear identification of the positions of the solitons, the method described in [27] was used.

as a starting point for studies in which Δ was varied in this range.

Starting from this idealized 29 row structure and decreasing the misfit one finds that the 29 row structure is stable down to about $\Delta_c' \approx 1.3$, at which point the soliton lattice disappears and the system spontaneously transforms into a defect-free structure with $n_y = 30$ rows again (Fig. 2). This value of Δ is to be compared with that for the reverse transition from 30 to 29 rows, which we recall occurs at $\Delta_c \approx 2.0$. Thus, with the standard Monte Carlo approach there is considerable hysteresis which precludes the accurate location of the transition point. Clearly, therefore a method is needed from which one can locate where the transition occurs in equilibrium.

Similar hysteresis is observed if one starts out from the 29 row structure but increases the misfit beyond $\Delta = 3$ (a case that has not been studied previously). As Fig. 2 shows, a transition occurs to structures with $n_y - 2 = 28$ rows (at about $\Delta \approx 4.1$). Unfortunately, there seem to be no unique candidates for stable structures having $n_y - 2 = 28$. Figure 4 displays four candidate structures that we have identified, each of which is at least metastable on simulation time scales. Depending on which of these 28 row candidates one takes, the transition from 28 to 29 rows on reducing the misfit occurs at anything between $\Delta = 3.2$ and $\Delta = 3.75$. As regards the nature of the candidate structures, in each case $2n_x = 216$ extra particles have to be distributed across the system. If we again keep the rows adjacent to the walls free of extra particles, the particle number per inner row becomes $n_x' = n_x + 2n_x/(n_y - 4) \approx n_x + 8.3$, that is, is noninteger. If we kept two rows adjacent to the wall rows free of extra particles, we would have nine extra particles per row, and thus this structure has been tried (this is configuration number 1 in Fig. 4). Another structure was obtained if we place four extra particles in the rows directly adjacent to the walls and eight extra particles in each of the 26 inner rows (configuration number 2). By energy minimization of a somewhat disordered structure resulting from a transition from 29 to 28 rows a structure was obtained which had nine solitons on one wall but only eight on the other wall (configuration number 3). Finally, another configuration with eight solitons on each wall (configuration number 4) was found. Note that the configurations shown in Fig. 4 are not the actual structures at $T = 1.0$ but the corresponding "inherent structures" found from the actual structures by cooling to $T = 0$, to clearly display where the solitons occur. Clearly, it again is a problem to (i) identify which of these 4 configurations with 28 rows is the stable one (at $T = 1.0$), and (ii) determine at which misfit the transition to the structure with 29 rows occurs. As we demonstrate below, both problems can be elegantly dealt with by employing the phase switch Monte Carlo method.

III. FREE ENERGY BASED SIMULATION METHODOLOGIES TO LOCATE TRANSITIONS BETWEEN IMPERFECTLY ORDERED CRYSTAL STRUCTURES

A. Thermodynamic integration

The general strategy of TI is to consider a Hamiltonian $\mathcal{H}(\lambda)$ that depends on a parameter λ that can be varied from a reference state (characterized by λ_0) whose free energy is known, to the state of interest (λ_1), without encountering phase transitions. The free energy difference ΔF can then be written as

$$\Delta F = F(\lambda_1) - F(\lambda_0) = \int_{\lambda_0}^{\lambda_1} d\lambda' \langle \partial \mathcal{H}(\lambda')/\partial \lambda' \rangle_{\lambda'}. \qquad (4)$$

For a dense disordered system (fluid or a solid containing defects), Schilling and Schmid [15,16] proposed to take as a reference state a configuration chosen at random from a well equilibrated simulation of the structure of interest, at values of the external control parameters for which one wishes to determine the free energy. Particles can be held rigidly in the reference configuration $\{\vec{r}_i^{\,\mathrm{ref}}\}$ by means of a suitable external potential. (We recall that a somewhat related TI scheme for disordered systems known as the "tethered spheres method" has already been proposed by Speedy [59].) When these external potentials act, the internal interactions can be switched off. In practice, one can use the following pinning potential $U_{\mathrm{ref}}(\lambda)$ to create the reference state, where r_{cut} is a parameter discussed below:

$$U_{\mathrm{ref}}(\lambda) = \lambda \sum_i \phi\left(\left|\vec{r}_i - \vec{r}_i^{\,\mathrm{ref}}\right|/r_{\mathrm{cut}}\right) \quad \text{with } \phi(x) = x - 1. \qquad (5)$$

Here it is to be understood that particle i is only pinned by well i at $\vec{r}_i^{\,\mathrm{ref}}$, and not by other wells. However, identity swaps need to be carried out to ensure the indistinguishability of particles. The free energy of this noninteracting reference system then is

$$F_{\mathrm{ref}}(\lambda) = \ln(N/V) - \ln[1 + (V_0/V) g_\phi(\beta\lambda)], \qquad (6)$$

where $\beta = (k_B T)^{-1}$, V_0 (in $d = 2$ dimensions) is $V_0 = \pi r_{\rm cut}^2$ and

$$g_\phi(a) = \frac{2}{\lambda^2}\left[\exp(a) - \sum_{k=0}^{2} e^k/k!\right], \tag{7}$$

for the choice of $\phi(x)$ written in Eq. (5).

Then intermediate models $\mathcal{H}(\lambda)$ to be used in Eq. (4) are chosen as

$$\mathcal{H}'(\lambda) = \mathcal{H}_{\rm int} + U_{\rm ref}(\lambda), \tag{8}$$

where $\mathcal{H}_{\rm int}$ describes interactions in the system, which then are switched on (if necessary, in several steps). The free energy contribution of switching on these interactions can easily be determined by a Monte Carlo simulation which includes a move that switches the interactions on and off. The logarithm of the ratio of how many times the states with and without interactions were visited gives the free energy contribution. The free energy difference between the intermediate model where particle interactions are turned on and potential wells are also turned on and the target system with particle interactions but without potential wells then is computed by TI, for which

$$\langle \partial \mathcal{H}_{\rm ref}(\lambda)/\partial\lambda\rangle = \left\langle \sum_i \phi\left(\left|\vec{r}_i - \vec{r}_i^{\ \rm ref}\right|/r_{\rm cut}\right)\right\rangle \tag{9}$$

needs to be sampled [15,16]. This method has been tested for hard spheres [15,16], including also systems confined by walls from which wall excess free energies could be sampled [60].

B. Phase switch Monte Carlo

The phase switch method [18–23] computes directly the relative probabilities of two phases, by switching between them and recording the ratio of the simulation time spent in each. This ratio directly yields their free energy difference ΔF via $\Delta F = \ln(A^{(1)}/A^{(2)})$. Here $A^{(1)}$ and $A^{(2)}$ are the times spent in the respective phases which are proportional to the statistical weight of each phase [9].

The power of the phase switch method derives from its ability to leap directly from configurations of one pure phase to those of another pure phase (Fig. 5), avoiding the mixed phase states which—when one or both phases are crystalline—can be computationally problematic (see Sec. A 1 of the Appendix). The leap is implemented as a suitable global Monte Carlo move. One starts out by specifying for each of the two phases of interest (labeled by index $\alpha = 1,2$) a reference configuration. This can be expressed as a set of $i = 1, \ldots, N$ particle positions $\{\vec{R}_i^{(\alpha)}\}$. Note that the specific choice of a reference configuration for phase α does not matter (at least in principle; see Appendix), it need only be a member of the set of pure phase configurations that "belong" to phase α. Thus, for example in the present case, a suitable reference configuration for the $n = 30$ row defect-free structure could simply be a typical configuration chosen from a simulation run on this structure. However, it could equally be a configuration in which all particles are at the lattice sites of this structure.

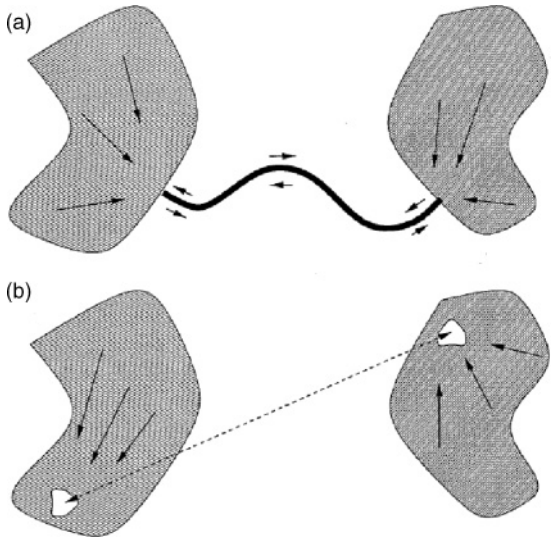

FIG. 5. Schematic comparison of (a) the standard method for linking phases via a sampling path and (b) the phase switch method. The blobs represent the set of values of some macroscopic property (e.g., order parameter or energy) associated with configurations belonging to two distinct phases ($\alpha = 1,2$). These pure phase states (having high probability) are separated by a "deep valley" in the free energy landscape corresponding to interfacial states having a very low probability. (a) In the standard strategy one uses extended sampling to negotiate the valley, by climbing down into it from one side and climbing up out of it on the other. (b) The idea of phase switch Monte Carlo is to "jump over the valley."

Given the two reference configurations, one can express the position vectors $\vec{r}_i^{(\alpha)}$ of each particle i in phase α as

$$\vec{r}_i^{(\alpha)} = \vec{R}_i^{(\alpha)} + \vec{u}_i, \tag{10}$$

where $\{\vec{u}_i\}$ is a set of displacement vectors which measure the deviation of each particle from the reference site to which it is nominally associated. Note that while there is a separate reference configuration for each phase, the single set of displacements is common to both phases.

Let us suppose the simulation is currently in phase $\alpha = 1$. Now the phase switch idea is to map the current configuration $\{\vec{r}_i^{(1)}\}$ of this phase onto a configuration of phase $\alpha = 2$ by switching the sets of reference sites from $\{\vec{R}_i^{(1)}\}$ to $\{\vec{R}_i^{(2)}\}$ but keeping the set of displacements $\{\vec{u}_i\}$ *fixed*. This switch can be incorporated in a global Monte Carlo move. Of course, in general the set of displacements that are typical for phase $\alpha = 1$ will not be typical displacements for phase $\alpha = 2$. As a consequence, in a naive implementation such a global move will almost always be rejected by the Monte Carlo lottery. This problem is circumvented by employing extended sampling methods [9,10,61] that create a bias which enhances the occurrence of displacements $\{\vec{u}_i\}$ for which the switch operation does have a sufficiently high Monte Carlo acceptance probability. Such states are called "gateway states" [18–22]: Crucially, they do not need to be specified beforehand; the system autonomously guides itself to them in the course of the biased sampling.

In practice, the bias is administered with respect to an "order parameter" M whose instantaneous value is closely related

to the energy cost of implementing the phase switch. One then introduces a weight function $\eta(M)$ into the sampling of the effective Hamiltonian which enhances the probability of the system sampling configurations for which the energy cost of the phase switch is low, thereby increasing the switch acceptance rate. Of course, the weight function $\eta(M)$ to be used is not known beforehand, and thus needs to be iteratively constructed in the course of the Monte Carlo sampling. One has a choice of ways of doing so: We have used the transition matrix Monte Carlo method [61–63] (see also the Appendix for implementation details). Alternative methods such as Wang-Landau sampling [64] or successive umbrella sampling [65] could also be applied.

Once a suitable form for the weight function $\eta(M)$ has been found, a long Monte Carlo run is performed, in the course of which both phases are visited many times. The statistics of the switching between phases is monitored by accumulating the histogram of M, which (as in all extended sampling methods) is corrected for the imposed bias at the end of the simulation. Doing so yields an estimate of the true equilibrium distribution $P(M)$, which in general exhibits a double peaked form (one peak for each phase). The free energy difference between the two phases is simply the logarithm of the ratio of the peak weights as described at the start of this section.

Of course, the above description was only intended to outline the phase switch strategy; more extensive implementation details are given in the Appendix. Additionally, the Appendix discusses how specific phenomena occurring in our model system have been handled.

IV. RESULTS

A. Free energy differences and computational efficiency

Figure 6 shows the absolute free energies in the *NVT* ensemble for the phase with 30 rows (and no defects) and the phase with 29 rows and the "soliton staircase" [Fig. 3(b)]

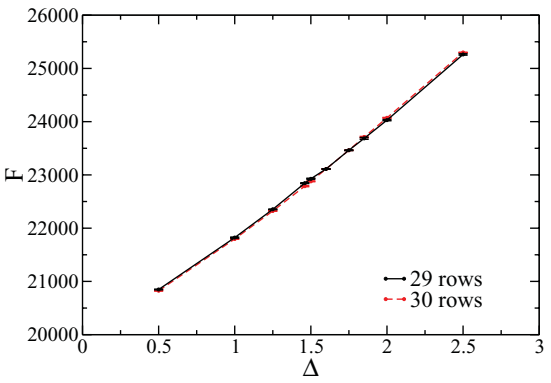

FIG. 6. (Color online) Absolute free energy F of systems of $N = 3240$ particles interacting with the potential given in Eq. (1) in an $L \times D$ geometry with $L = 108a$, a being the lattice spacing, and periodic boundaries in the x direction, confined by two rows of fixed particles on either side in the y direction (Fig. 1), as a function of the misfit Δ [see Eq. (3)]. Two structures are compared: (i) a (compressed) triangular lattice with $n_y = 30$ rows containing $n_x = 108$ particles per row; (ii) a lattice with $n_y = 29$ rows and corresponding soliton staircase [Fig. 3(b)].

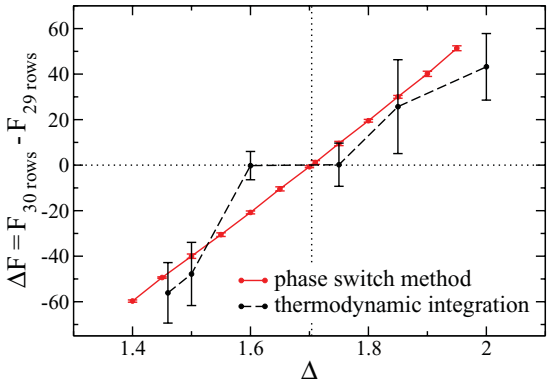

FIG. 7. (Color online) Free energy differences between structures with 29 and 30 rows plotted versus the misfit Δ. Both results obtained from TI and from the phase switch method are shown, as indicated.

as a function of the misfit Δ, as obtained from the TI method (Sec. III A). One sees that these free energies are very large (note the ordinate scale) and vary rather strongly with Δ. However, the free energy curves with these two structures are barely distinct from each other, and hence a very substantial computational effort is needed to locate, with meaningful accuracy, the intersection point marking the equilibrium transition between $n = 30$ and $n = 29$ rows.

Figure 7 plots the free energy difference ΔF versus the misfit, comparing the results from the TI method (points with error bars) with the results from the phase switch method, and focusing on the region near the transition. One can see that within the errors the results of both methods agree very well with each other, although for the TI method the error is at least an order of magnitude larger than that of the phase switch simulations. We note that the predicted equilibrium value of the misfit at the transition point ($\Delta_t \approx 1.7$) falls well within the hysteresis loop of Fig. 2.

Since the absolute free energies are of the order of 20 000 (for our system with $N = 3240$ particles) but in the region of interest free energy differences are of order ± 60 only, we have that the relative error $\delta F/F$ is of order $1/500$. Thus, for TI, it would be difficult to bring the error bars down further in Fig. 7. The error bars for the phase switch simulation were computed from the results of four independent runs for each value of the misfit and are hardly visible on the scale of Fig. 7.

In addition to this significant difference with respect to the size of the statistical errors, phase switch Monte Carlo also outperformed the TI method with respect to the necessary investment of computer resources. In order to obtain a suitable weight function for our system, at a certain value of the misfit, we let the simulation run for about 15 million steps (each step consisting of one sweep of local moves and one attempt to switch the phases). On the ZDV cluster of the University of Mainz, this takes about 4.5 days on a single core (though in hindsight we could have got away with a less smooth weight function, further reducing the computing time of this step). Having determined the weight function, we initiated four production runs for every value of the misfit. These runs needed again 10 million steps each (i.e., about 3 days each) in order to perform a sufficient number of phase switches to yield results of the desired precision. Overall, then, computing each

point of the free energy difference curve of Fig. 7 by phase switch took about 16.5 days of CPU time.

In contrast to this, the TI method required a calculation not only of the free energy difference in which we are interested, but of the free energy difference along the path of the TI, gradually switching off the wells of attraction used there, and of the free energy difference between the state where the particle interactions were turned on and the state where they were turned off. This needs to be done for both phases separately. It is therefore not surprising that considerably more CPU time was needed: Roughly 250 days of CPU time was invested for each phase and for each value of the misfit to obtain the absolute free energy (again converting units to a single core). Thus, each of the 12 values of free energy differences needed for Fig. 7 required 500 days (rather than 16.5 days), that is, a factor of 30 more computational effort. However, if we were to bring the statistical errors of the TI method a factor of 10 down (to make it comparable to the phase switch method), we would need another factor of 100 in computer time; the benefit of using the (clearly much more powerful) phase switch approach hence amounts to a gain of the order of 10^3 in computational resources. Of course, this is no surprise when we remember that the free energy differences of interest are only of the order of (1/500) of the total free energies for the present model system.

B. Ensemble inequivalence

We turn now to a discussion of a puzzling aspect of the physics, namely the fact that we treat here a first-order structural phase transition obtained by variation of the distance D between the walls formed by the rigidly fixed particles, that is, an *extensive* rather than an *intensive* thermodynamic variable. If we were concerned with the study of a vapor to liquid transition of a fluid in such a geometry, the proper way to locate a discontinuous transition is the variation of the intensive variable thermodynamically conjugate to D, which is the normal pressure p_N (force per area acting on the walls). (In the following the index N will be omitted. Of course, at fixed lateral dimensions L a variation of D is equivalent to a variation of the volume V.)

To fix ideas, we remind the reader about this classical vapor-liquid problem in Fig. 8(a): In the NpT ensemble, we would have a jump in volume $V = LD$ from $V_v = LD_v$ (density of the vapor $\rho_v = N/V_v$) to $V_\ell = LD_\ell$ (density of the liquid $\rho_\ell = N/V_\ell$) at the transition pressure p_t. If we work in the conjugate NVT ensemble, of course, the behavior simply follows from a Legendre transform, the volume jump from V_v to V_ℓ translates into a horizontal plateau at $p = p_t$, and any state of this plateau is a situation of two-phase coexistence, as schematically indicated in Fig. 8(a).

Of course, it is also possible to consider the present transition between a state of n rows to $n-1$ rows in the NpT ensemble [Figs. 8(b) and 9(c)]. Then it is clear that the transition will show up as a jump in the thickness D from $D_n(= na_n)$ to $D_{n-1}\,(= (n-1)a_{n-1})$, where a_n, a_{n-1} are the (average) distances between the lattice rows (or lattice planes, in three-dimensional films, respectively). The corresponding phases of the n-layer state and $(n-1)$ layer state are indicated below the isotherm in the $(p-D)$ plane schematically.

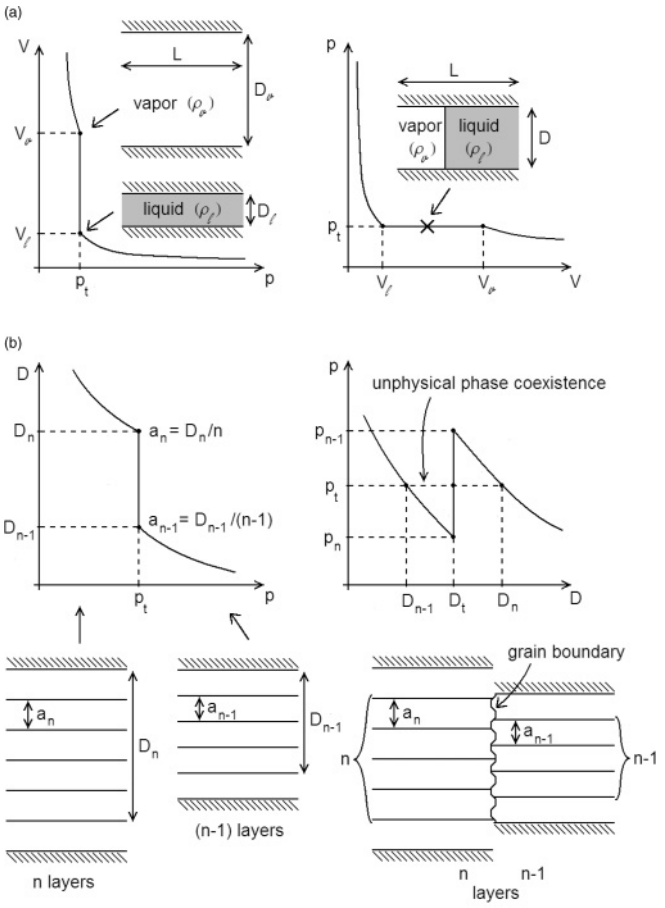

FIG. 8. Schematic description of phase transitions in thin films of thickness D in the conjugate NpT (left) and NVT (right) ensembles, for the case of a vapor-liquid transition (a) and the present transition where the number of rows is reduced ($n \to n-1$) when either the (normal) pressure p increases (left) or the thickness decreases (right). Note that in the latter case two-phase coexistence is possible for the vapor-liquid transition, but not for the transition where the number of rows parallel to the boundaries change. For further explanations, see text.

However, one simply cannot construct a state of two-phase coexistence out of these two "pure phases" at a value of D intermediate between D_{n-1} and D_n: Locally the n-layer state requires a thickness D_n, the $(n-1)$ layer state a thickness D_{n-1}, so one would have to "break" the walls. Of course, it is not just sufficient to have a state with n layers separated by a grain boundary from a state with $(n-1)$ layers at the same value of D: These domains are *not* the coexisting pure phases in the NpT ensemble.

So the phase coexistence drawn (horizontal broken curve) in Fig. 8(b) is unphysical, it requires a state where the constraining walls were broken. Requesting the integrity of the walls is a global constraint which makes phase coexistence in the standard sense impossible for the present transitions. Thus, the rule that the different ensembles of statistical mechanics yield equivalent results in the thermodynamic limit is not true for the present system; in the transition region $D_{n-1} < D < D_n$ the NVT ensemble and the NpT ensemble are *not equivalent*.

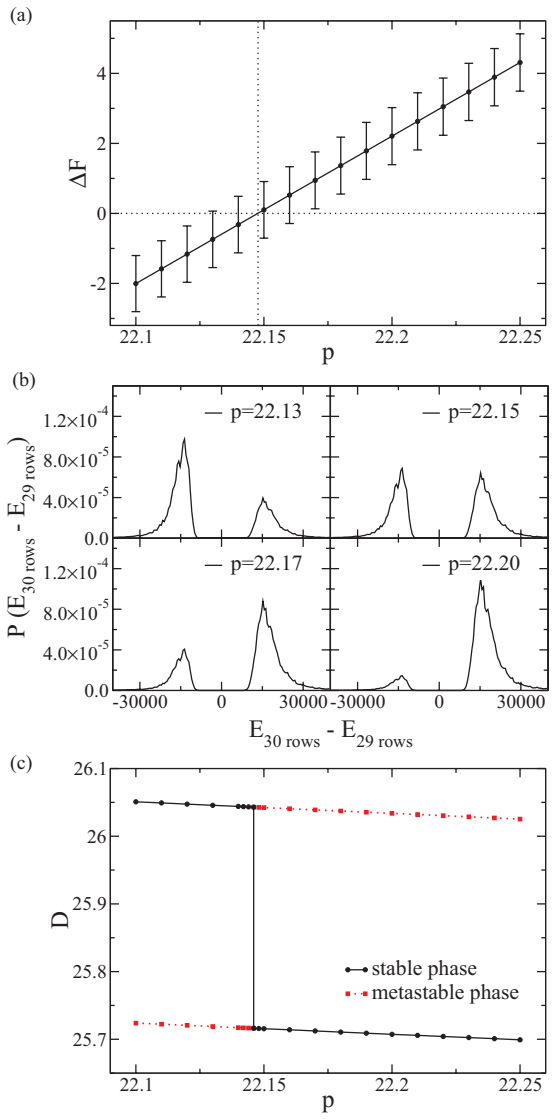

FIG. 9. (Color online) (a) Free energy difference ΔF for the transition from $n = 30$ to $n = 29$ rows as a function of pressure. (b) The distribution of the internal energy difference between the two phases $p(E_{30\text{ rows}} - E_{29\text{ rows}})$ at fixed $\{\vec{u}\}$. Curves for four pressures near and at the transition pressure $p_t = 22.146 \pm 0.015$ are shown, as generated via histogram reweighting. The simulation was run at a pressure of $p = 22.13$. (c) System length D as a function of pressure. Clearly, the curve for the stable phase exhibits a jump at the transition pressure. Statistical errors are smaller than the symbol sizes.

Actually, this is not the first time that such an ensemble inequivalence has been pointed out. A case much discussed in the literature is the "escape transition" of a single polymer chain of N beads grafted at a planar surface underneath a piston held at a distance D above the surface to compress the polymer [66–72]. For pressures $p < p_t$ (where the piston is at distance $D_{t,1}$) the chain is completely confined underneath the piston (which has the cross section of a circle in the directions parallel to the surface), while for $p > p_t$ the chain is (partially) escaped into the region outside of where the piston acts (the piston distance at p_T jumps to a smaller value $D_{t,2}$). When we use instead D as the control variable, again a sharp transition occurs (for $N \to \infty$) at some intermediate value D_t ($D_{t,2} < D_t < D_{t,1}$), since obviously it is simply inconceivable to have within a single chain phase coexistence between states "partially escaped" and "fully confined," since these states are defined only via a global description of the whole polymer chain.

Another case where transitions of the number n of layers in layered structures in thin films occur is the confinement of symmetric block copolymer melts (which may form a lamellar mesophase of period λ_0 in the bulk) in thin films between identical walls [73–76]. When then the thickness D of such films is varied, one observes experimentally discontinuous transitions in the number n of lamellae parallel to the film [74,75]. However, when one considers block copolymer films on a substrate and does not impose the constraint of a uniform thickness but rather allows the upper surface to be free, then indeed mixed phase configurations of a region where $n - 1$ layers occur (and take a thickness D_{n-1}) and of a region where n layers occur (and take a thickness D_n) are conceivable [76] and have been observed (see, e.g., [77]). In summary of these remarks, we note that it is not uncommon that global geometric constraints may destroy the possibility of phase coexistence.

In view of the above discussion, it is of interest also in the present case to investigate the use of the (normal) pressure p (instead of the strip width D) as the control variable. Taking, in the spirit of the general remarks on the phase switch method, the appropriate phase switch energy cost as an order parameter M, we can sample the probability distribution function $p(M)$ which exhibits two well-separated peaks of generally different weights. These peaks are even more clearly visible in the distribution of the energy difference $p(E_{30\text{ rows}} - E_{29\text{ rows}})$ at fixed $\{\vec{u}\}$ as the order parameter M is related to this energy difference via a logarithmic function [cf. Eq. (A2)]. The transition pressure p_t is that for which the peaks have equal weight (Fig. 9) and can be determined accurately via histogram reweighting. From this we estimate that $p_t = 22.146 \pm 0.015$. At the transition, the measured misfit Δ jumps from $\Delta_1 = 1.913 \pm 0.043$ (for $n = 30$) to $\Delta_2 = 1.503 \pm 0.046$ (for $n = 29$). Interestingly, the misfit where the transition in the NVT ensemble occurs ($\Delta_t \approx 1.71$) is just the average of these two values.

C. Comparison of competing candidate structures

Returning again to the NVT ensemble, we now consider the transition from states with 29 layers to states with 28 layers. We recall (Fig. 4) that several different candidate structures do exist, and it is not at all clear *a priori*, which of them should be favored. Again, the phase switch Monte Carlo is a convenient tool to solve such a problem: We utilize reference states from all four of the candidate structures having $n = 28$ (as shown in Fig. 4) and calculate the free energy difference ΔF between the (unique) structure with $n = 29$ and these four candidates.

The results (Fig. 10) clearly show that configuration numbers 1 and 3 are metastable, because they have distinctly higher free energy differences throughout the range of Δ than configuration numbers 2 and 4, which practically coincide. In fact, this coincidence between the free energies of configuration numbers 2 and 4 is not accidental: A closer evaluation of their time evolution shows that they transform

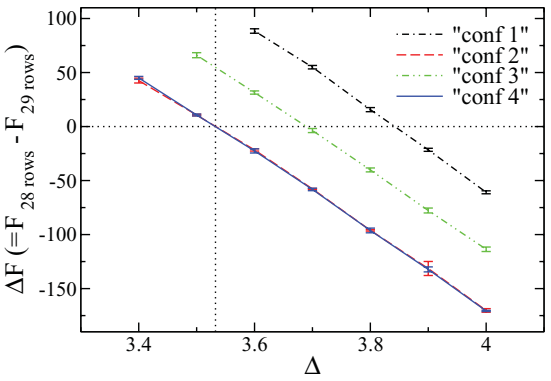

FIG. 10. (Color online) Free energy differences between various structures with $n = 28$ rows and the structure with $n = 29$ plotted vs the misfit Δ. As configuration numbers 2 and 4 turned out to be the same, their free energy curves fall on top of each other.

into each other via sequences of "easy" local moves, and although the instantaneous snapshot pictures reproduced in Fig. 4 were different, they do not belong to different phases in a thermodynamic sense.

It is also interesting to note that the conclusion that structure number 2 is the stable one would not have been obtained by a simple comparison of the internal energies of the four structures: Indeed, configuration number 2 has the highest energy of all four structures.

Thus, entropy matters in soft crystals, such as those studied here.

V. CONCLUDING REMARKS

The principal findings of our study are twofold. (i) We have performed a thorough test of the suitability of the phase switch Monte Carlo method for the task of determining the relative stability of imperfectly ordered structures of typical soft-matter systems, where one must deal with systems which have at least one very large linear dimension. For such a test, it is crucial to provide full information on the model that is studied and to give a careful description of the method and its implementation. Moreover, we have studied precisely the same model system by a TI method, thereby allowing the first like-for-like comparison between the two approaches. We find that the results from both methods are compatible, but the accuracy that can be achieved using phase switch MC is at least an order of magnitude better (Fig. 7), despite requiring a factor of 30 less computational time.

The reasons for this efficiency gain can be appreciated from a glance at Fig. 6: The absolute free energies of our system of 3240 particles vary from about 22 000 to 24 000 (in suitably scaled units), for a misfit parameter Δ varying from 1 to 2, while the free energy difference between the two states that we wish to compare vary only from -60 to $+60$ in the same range. These numbers illustrate vividly the basic concept of phase switch Monte Carlo: One does better in focusing directly on the small free energy difference between the states that one wishes to compare, rather than extracting them indirectly by subtracting two measurements of large absolute free energies. Thus (in the present context at least), phase switch Monte Carlo seems a much more powerful approach than TI. In fact, if one were to try to bring the errors of the TI method down by an order of magnitude—to make the error bars of both methods in Fig. 7 comparable—one would have to invest a factor of 3000 more computational time. We feel that the case of relatively small free energy differences between competing phases and/or structures is rather typical for soft matter systems. Indeed, for many soft matter systems, such as block copolymer mesophases, the relative magnitude of free energy differences is much less than the factor of about $1/500$ encountered here, and hence such problems could never be tackled successfully with TI methods since the computational effort to reach the requisite accuracy would be prohibitive.

The first problem to which phase switch Monte Carlo was applied (in the form of the "Lattice-switch" method) evaluated the free energy difference of perfectly ordered face-centered cubic and hexagonal close-packed crystals. Such an application might be regarded as a somewhat special case due to the perfect long-range order in these defect-free crystals. However, the present work shows that the method can equally be applied to imperfectly ordered crystals. Here, due to the confinement by structured walls together with a misfit between the distance between the walls and the appropriate multiple of the distance between the lattice rows, somewhat irregular long-range defect structures form along the walls ("soliton staircase"). Additionally, several similarly ill-crystallized structures can present themselves as candidates for the optimal structure (Fig. 4). It would be absolutely impossible to identify which is the equilibrium structure and which structures are only metastable without the phase switch Monte Carlo method (Fig. 10).

We note that the model system that we have chosen to study (Fig. 1) could also be experimentally realized in colloidal dispersions, though with some effort: Colloids coated with polymer brushes experience a short-ranged, almost hard-sphere-like, repulsive effective potential, and bringing them to an interface where water is on top and air is below, rather perfect two-dimensional crystals with triangular lattice structure form. Interference of strong laser fields can be used to create a periodic confining potential, through which the misfit and thus the crystal structure can be manipulated. We hope that our study will solicit some corresponding experimental studies to show that the proposed transitions in the number of rows in these crystalline strips actually occur.

(ii) Our second main finding is that this type of system has an interesting physical property, namely the inequivalence between conjugate ensembles of statistical mechanics. When we fix the distance D between the confining "walls," the total particle number N and the total (two-dimensional) "volume" V of the system, we realize the NVT ensemble. When one studies first order transitions in the bulk using such an ensemble containing two extensive variables (N, V), a first order transition normally shows up as a two-phase coexistence region (e.g., at fixed N the two-phase coexistence extends from V_I to V_{II}). However, here such a two-phase coexistence is not possible (Fig. 8), and thus one has the unusual behavior that at the equilibrium in the "constant D" ensemble the conjugate intensive variable (the normal pressure p_N, as well as the stress σ; cf. Fig. 2) exhibit jumps (in Fig. 2, we display the hysteresis loops, but the positions of the jumps in equilibrium can be inferred from $\Delta F = 0$ in Figs. 7 and 10,

respectively). When we use a "constant p" ensemble (which is physically reasonable if the confinement of the crystal is effected mechanically in a surface force apparatus), it is the "volume" (i.e., the distance between the walls D) which jumps from D_I to D_{II} at a well-defined transition pressure (cf. Figs. 8 and 9).

One should not confuse this ensemble inequivalence with the well-known ensemble inequivalence between NVT and NpT ensembles in systems where N is finite: In the latter case, the ensemble inequivalence is dominated by interfacial contributions (in the NVT ensemble, when $V_I < V < V_{II}$, the system is in a two-phase configuration, as suggested for $V \to \infty$ by the "lever rule," but for finite V the relative contribution due to the interface between the coexisting phases dominate the finite size effects). However, for $V \to \infty$ these interfacial effects become negligible; the properties in the two conjugate ensembles are just related by the appropriate Legendre transformation. This equivalence between the ensembles holds also for liquid-vapor or liquid-liquid unmixing under confinement in a thin film geometry: When D is finite and the particle number $N \to \infty$, that is, the lateral linear dimensions become macroscopic, we still have ordinary two-phase coexistence in the thin films (cf. Fig. 8). The ensemble inequivalence in the present system arises from the lack of commensurability between the thickness D of the slit and the appropriate multiple of the lattice distance. At a transition pressure p_t in the 3 ensemble we inevitably have different distances D_I, D_{II} between the walls for the two phases I, II. Thus, they cannot coexist for any uniform value of D. Similar phenomena (where the number of layers of a layered lamellar structure confined between walls exhibits jump discontinuities when D is varied) are already known, both experimentally and theoretically, for block copolymer mesophases, but the aspect of ensemble inequivalence has not been addressed, to our knowledge, in these systems studied here.

ACKNOWLEDGMENTS

One of us (D.W.) acknowledges support from the Deutsche Forschungsgemeinschaft (DFG) under Grant No. TR6/C4 and from the Graduate School of Excellence "Material Science in Mainz (MAINZ)." She is also grateful to the Department of Physics, University of Bath (U.K.), for its hospitality during an extended research stay under the auspices of the visiting postgraduate scholar scheme. We thank P. Virnau, T. Schilling, F. Schmid, and I. K. Snook for helpful discussions and advice.

APPENDIX

Here we provide an extended description of the implementation of phase switch Monte Carlo, concentrating on implementation details at a level suitable for a new practitioner.

1. Implementation details for the phase switch method

In order to calculate the free energy difference between two phases in a single simulation run, the two phases have to be linked by a sampling path. In many popular approaches, a direct path between the two phases is constructed in the form of a continuous set of macrostates associated with the values of some order parameter which distinguishes one phase from the other (common examples are the total energy or density of a fluid). This path traverses mixed phase (interfacial) states [78] and is negotiated using some form of extended sampling to overcome the free energy (surface tension) barrier associated with the interfacial states. One way to do this is the multicanonical method [79]. Alternatively, one can directly measure free energy differences between successive points along the path as is the case in the successive umbrella sampling technique [65].

In many cases utilizing an interphase path that encompasses interfacial states works well, particularly for fluid-fluid transitions or lattice models of magnets. However, in other cases such a path can be problematic [9]. For example in the case of solid-liquid coexistence, a connecting path will typically run from a crystalline phase through several different distinct states including droplets of liquid in a crystal, a slab configuration and crystalline droplets in a liquid before finally reaching the pure liquid phase [80]. In such cases the identification of a suitable order parameter to guide the system smoothly from one pure phase to the other can be difficult, and as a result the system may experience kinetic trapping (e.g., in defective crystalline states).

Thus, it is highly desirable to have a method which can directly "leap" between the two pure phases (which we label α, with $\alpha = 1,2$), avoiding the problematic mixed phase states. If the system jumps back and forth between these phases a sufficient number of times within one simulation run, the relative probability with which the system is found in each of them directly yields the free energy difference between these phases via $\Delta F = -\ln(\frac{P^{(\alpha=1)}}{P^{(\alpha=2)}})$. The phase switch method achieves this by supplementing standard local particle displacement moves (and in the case of a simulation in the NpT ensemble, moves which scale the volume of the simulation box) with moves that switch the system from one phase directly into the other phase. This switch is facilitated by the *representation* of particle configurations in the two phases. Specifically, we associate a fixed reference configuration $\{\vec{R}^{(\alpha)}\}$ with each phase. The reference configuration is an arbitary configuration drawn from the set of configurations that are identifiable as "belonging" to phase α. We then associate each particle with a unique site of the reference configuration, allowing us to write its position $\vec{r}_i^{(\alpha)}$ in terms of the displacement $\vec{u}_i$ from its reference site:

$$\vec{r}_i^{(\alpha)} = \vec{R}_i^{(\alpha)} + \vec{u}_i. \tag{A1}$$

Note that while there are two reference configurations (one for each phase), the phase switch method only considers one set of displacement vectors which are regarded as common to both phases.

Suppose we are currently in phase $\alpha = 1$, so that the particle coordinates are $\vec{r}_i^{(1)} = \vec{R}_i^{(1)} + \vec{u}_i$. For local moves in this phase we update particle coordinates (in the manner to be described) which, owing to reference sites being fixed, is equivalent to updating the displacement vectors. For a phase switch to phase $\alpha = 2$, we propose a new configuration which is simply formed by substituting the reference sites of phase $\alpha = 1$ with those of phase $\alpha = 2$. Thus, the proposed configuration is $\{\vec{r}_i^{(2)}\} = \{\vec{R}_i^{(2)}\} + \{\vec{u}_i\}$. If this switch is accepted, that is, if the resulting

configuration of phase $\alpha = 2$ is energetically acceptable, the simulation will continue to run in phase $\alpha = 2$, again recording the displacements of all of the particles from the reference sites of phase $\alpha = 2$, and proposing switches back to phase $\alpha = 1$. In this way the system switches repeatedly back and forth between the phases, allowing one to record the relative probability of finding the system in each phase.

The switch operation leaves open how one chooses the lattice-to-lattice mapping between reference sites in the two phases, that is, the relationship between the pairs of sites $\vec{R}_i^{(1)}$ and $\vec{R}_i^{(2)}$. In fact, it turns out to be beneficial in terms of the efficiency of the method to choose this mapping such as to maintain any local structural similarities that may exist in the two phases. Thus, having specified the reference sites for one phase by labeling all the lattice sites with the index i, one should consider how each lattice site transforms under the structural phase transition, and assign the same index to the corresponding lattice site in the other phase. In the present model some particles (those not near the wall or the solitons) do not see a significant change to their local environment under the phase transition and so the mapping is straightforward. Only the particles redistributed from near the walls to the solitons see a significantly new environment and for pairs of these particles it is essentially arbitrary which index they receive.

Now generally speaking the displacement vectors that characterize phase $\alpha = 1$ are not typical of phase $\alpha = 2$ and thus it will not be energetically acceptable to perform the switch from typical configurations of phase $\alpha = 1$. To deal with this, one introduces a bias in the accept/reject probabilities for local moves that enhances the probability of displacements being generated in phase $\alpha = 1$ for which the phase switch to $\alpha = 2$ *is* energetically acceptable. The obvious observable to which the bias should be administered is a quantity related to the instantaneous energy cost of the switch, since this measures how likely it is to be accepted. We have employed the switch energy order parameter M described in Ref. [22], which for switches from phase $\alpha = 1$ to $\alpha = 2$ is defined as follows:

$$M^{(1)\to(2)}(\{\vec{u}\}) = \mathrm{sgn}(\Delta \mathrm{E}^{(1)\to(2)}) \cdot \ln(1 + |\Delta \mathrm{E}^{(1)\to(2)}|), \quad \text{(A2)}$$

where

$$\Delta E^{(1)\to(2)} = \left(E^{(2)}(\{\vec{u}\}) - E^{(2)}_{\mathrm{ref}}\right) - \left(E^{(1)}(\{\vec{u}\}) - E^{(1)}_{\mathrm{ref}}\right), \quad \text{(A3)}$$

where $E^{(\alpha)}_{\mathrm{ref}}$ is the energy of the reference configuration in phase α, and $E^{(\alpha)}(\{\vec{u}\})$ is the energy in phase α, found by applying the displacement vectors $\{\vec{u}\}$ to the reference configuration $\{\vec{R}^{(\alpha)}\}$. An obvious substitution gives the order parameter for the switch from $\alpha = 2$ to $\alpha = 1$. Note that an important feature of this definition of this order parameter is the logarithm which ensures that the binning of the weight function is finer for small values of the energy difference and thus serves to ensure that the simulation can cover the entire range of M smoothly.

Now, when implementing local moves for particles, we consider not just the energy cost of the move within the current phase, but also the change in M associated with the local move via a weight function $\eta(M)$. The acceptance criterion for the local move is therefore given by

$$p^{(\alpha)}(\{\vec{u}\} \to \{\vec{u'}\}) = \min(1, \mathrm{e}^{-\beta(\mathrm{E}^{(\alpha)}(\{\vec{u'}\}) - \mathrm{E}^{(\alpha)}(\{\vec{u}\})) + \eta(\mathrm{M'}) - \eta(\mathrm{M})}). \quad \text{(A4)}$$

Note that $E^{(\alpha)}(\{\vec{u'}\})) - E^{(\alpha}(\{\vec{u}\})$ is the energy difference due to the move in the phase α that is currently being simulated. The energy difference in the other phase is only needed for the computation of the new order parameter M' and therefore for the weights $\eta(M')$ associated with the move.

Phase switches are generally only accepted from states in which M is small, the so-called gateway states. One instance in which M becomes small is if the displacement vectors are themselves small, that is, if all particles are sitting close to their reference positions in both phases. Another instance is if there is a high degree of structural similarity among the phases, so that the displacements of many of the particles in one phase are typical of the displacements in the other phase. Note that one does not need to know or specify the gateway states to use the method. They are sought out automatically when one biases to small values of M.

The acceptance criterion for a phase switch from $\alpha = 1$ to $\alpha = 2$ itself reads

$$p^{(1)\to(2)}(\{\vec{u}\}) = \min(1, e^{-\beta(E^{(2)}(\{\vec{u}\}) - E^{(1)}(\{\vec{u}\}) + \omega^{(2)} - \omega^{(1)})}), \quad \text{(A5)}$$

and similarly for the reverse switch. This phase switch also includes a weight ω to ensure that it occurs with a sufficiently high probability in both directions. Note that since the phase switch move alters the absolute particle coordinates, the associated energy change enters the switch acceptance criterion. We therefore chose the weights ω in such a way that $\omega^{(2)} - \omega^{(1)} = E^{(1)}_{\mathrm{ref}} - E^{(2)}_{\mathrm{ref}}$, ensuring that a phase switch is always accepted if all particles are sitting on their reference positions despite the fact that the energies of the two phases might differ significantly. In the case of phase switch simulations in the *NpT* ensemble, an additional volume scaling must also be taken into account (see below).

Once suitable weights have been determined (see Sec. A 2 of the Appendix), one samples the statistics of the two phases by accumulating a histogram of the biased order parameter distribution $\tilde{P}(M)$. At the end of the simulation, the effects of the weights are unfolded from this distribution in the standard manner for extended sampling [9] to find the equilibrium distribution $P(M)$. Close to a phase transition, this distribution will exhibit two well-separated peaks, whose areas yield the free energy difference as described above. An example is shown in Fig. 11(a). Also shown in Fig. 11(b) is the distribution of the instantaneous energy change under the switch $E^{(\alpha')}(\{\vec{u}\}) - E^{(\alpha)}(\{\vec{u}\})$, which similarly shows two peaks, one for each phase.

With regard to the choice of reference configuration in each phase, in principle, this can be an arbitrary configuration belonging to that phase. In practice, however, for crystalline systems one finds that the degree of weighting required to access the gateway states can be reduced by choosing a reference configuration which is a perfect lattice. For more general system, for example, those with crystalline disorder, or for fluids it may be advantageous to try to ensure that the particles are not sitting too close to each other (e.g., by energy minimization of the configuration [21]), since particles which

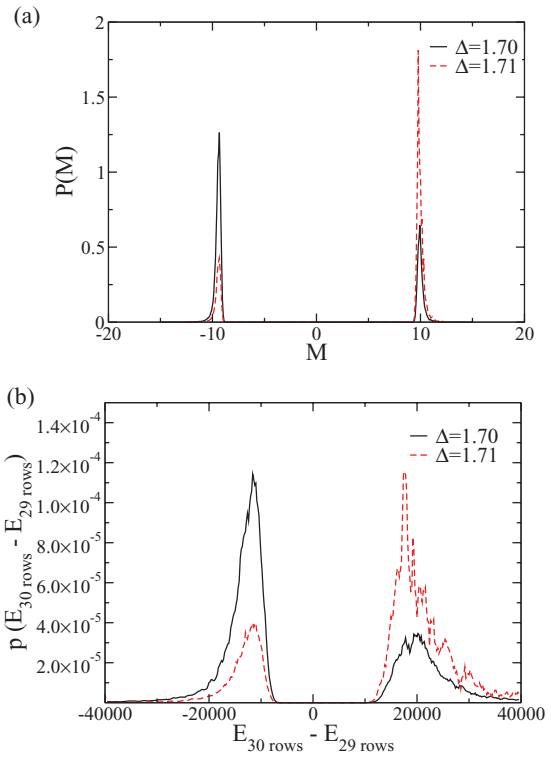

FIG. 11. (Color online) (a) The order parameter distribution $p(M)$ for simulations at $\Delta = 1.70$ and $\Delta = 1.71$ carried out in the *NVT* ensemble. (b) For comparison the same distribution is plotted against the internal energy difference between the two phases for fixed $\{\vec{u}\}$. The order parameter M is deduced from this energy difference $E_{29\text{ rows}} - E_{30\text{ rows}}$ via the definition given in Eq. (A2).

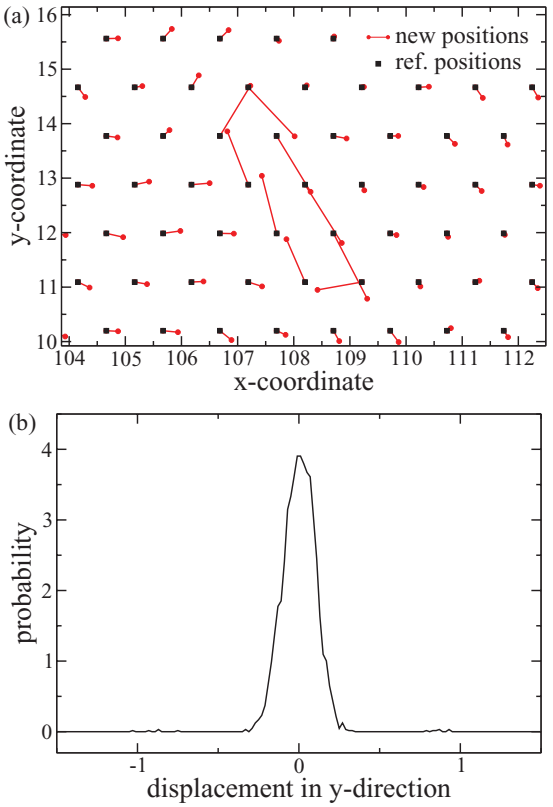

FIG. 12. (Color online) (a) A section of a configuration that includes particles which have swapped positions in the phase with 29 rows. Black squares denote the reference configuration, red (gray) lines are the displacement vectors associated with the reference positions, and red (gray) dots are the new positions. This simulation was carried out with 3240 particles at a misfit of $\Delta = 1.70$ in an *NVT* simulation with 1280 bins for the weight function. (b) Typical histograms of the particle displacements in the y direction. The (almost completely invisible) very small peaks at about $+1$ and -1 correspond to particles which have swapped their positions.

are in close proximity reduce the number of gateway states significantly. (We note in passing that for fluid systems [22] one requires special approaches to guide particles to the gateway states that we do not discuss here as they were not necessary for our system.)

With regard to the phase switch simulations of the present model of two-dimensional colloids in confinement, we mention a rare problem that appeared in our simulations of the 29 row system. This involved sets of particles on neighboring lattice sites in adjacent rows jumping between rows during the simulation, creating in the process a ring of particles which occupy each others' positions [cf. Fig. 12(a)] and remain there. This occurrence is primarily a feature of the two-dimensional nature of our system, and the well-known "softness" of two-dimensional crystals. When it occurs it interferes with the operation of the phase switch method because the weight function is not designed to deal with it, so one is prevented from reaching the gateway states. Although one can envisage methods for solving this problem along the lines of those used in fluids [22], our solution to the problem was to simply suppress it. A measurement of the distribution of displacements in the y direction is shown in Fig. 12(b) and shows that preventing particles from fluctuating any further in the y direction than $\Delta y = 0.5$ introduces a negligible constraint with regard to their natural fluctuations (and hence on free energy measurements). Doing so cured the problem of rare lattice site swaps.

Finally, we outline briefly how to apply the phase switch method in the *NpT* ensemble. The advantage of the *NpT* ensemble is that the results obtained at one pressure can easily be extrapolated to other values of the pressure by standard histogram reweighting methods. The difference between the *NVT* and the *NpT* ensemble in this case is that additional volume moves have to be carried out in the *NpT* ensemble. In such moves, all particle coordinates are scaled (along with the box) in both phases in the standard way [6,22]. Additionally, it can prove useful to combine the phase switch move itself with a volume scaling move if the equilibrium densities of the two phases differ from each other as it was the case for our system. For details on the underlying statistical dynamics and acceptance probabilities, see Ref. [22]. The problem of particles switching their positions and thus creating configurations which prevented any further phase switches from being accepted did not occur in the case of simulations in the *NpT* ensemble for our system. We obtained (within the error bars) the same free energies whether or not we restricted the movement of the particles in the y direction in the way we had to restrict them in the *NVT* ensemble.

2. Implementation details for the transfer matrix method

The choice of method for determining the weight function $\eta(M)$ that connects the configurations of high statistical weight to the gateway states is to some extent a matter of personal taste. A number of approaches exist such as the Wang-Landau method [64] or successive umbrella sampling [65]. In this work, we have found the transition matrix method to be a particularly efficient means of determining a suitable weight function. The transition matrix method has the advantage that—similar to the Wang-Landau sampling—the weights can be updated "on the fly" throughout the simulation, allowing the simulation to explore an ever wider range of values of the order parameter M as the weight function evolves, until it eventually encompasses the gateway states of low M. Once this has been achieved, one can cease updating the weight function and perform a simulation run with a constant weight function. An advantage of the transition matrix method over Wang-Landau sampling is that it collects equilibrium data from the outset of the simulation, whereas Wang-Landau only provides equilibrium estimates after a number of preliminary iterations.

The general idea of the transition matrix method for determining weight functions is to record the acceptance probabilities of all attempted transitions and extract the ratio of the states' probabilities from it. As all attempted transitions contribute to the weight function, including those that were rejected, the weight function can be built up rather quickly. The details of the implementation are as follows and can also be found in [21,22,61] and the references given therein.

To implement the transition matrix method, the range of the order parameter M, for which a weight function is desired, is divided into a number of bins. In our case this range corresponds to the values of M that lie between the peaks in $P(M)$ which correspond to the two phases [cf. Fig. 11(a)]. A good choice for the binning of the order parameter is to choose the bins in such a way, that the weight difference between adjacent bins satisfies [22] $|\eta(M_{i+1}) - \eta(M_i)| < 2$. Then, for every attempted move the acceptance probability p (which is calculated anyway for use in the Metropolis criterion) is stored in a collection matrix C:

$$C(M \to M') \Rightarrow C(M \to M') + p. \tag{A6}$$

At the same time, the probability for rejecting the move and thereby keeping the current value of the order parameter is also stored:

$$C(M \to M) \Rightarrow C(M \to M) + (1 - p). \tag{A7}$$

It is important to note that these probabilities p are the "bare" acceptance probabilities and do not include any weights.

The transition probabilities are then simply calculated by a normalization of the values in the collection matrix, with the sum on the right hand side including all possible states to which the system can jump from a given state:

$$T(M \to M') = \frac{C(M \to M')}{\sum_k C(M \to M_k)}. \tag{A8}$$

In the most general case, this method would create an $N \times N$ matrix, N being the number of bins or values of the order parameter M. In order to derive the correct probability distribution from such an $N \times N$ transition matrix, it is necessary to compute the eigenvector to the largest eigenvalue of this matrix. However, it is not necessarily required to know the exact probability distribution in order to create a weight function that will work sufficiently well. Therefore, it is possible to take only those transitions occurring between neighboring bins of the order parameter into account when computing the weight function. In terms of the transition matrix, this means that only the diagonal elements—corresponding to transitions from a state to itself—and the first off-diagonal elements—corresponding to transitions from one state to the adjacent ones—are taken into account. Using this approach the weight function can be calculated quite easily without the need to compute eigenvalues or eigenvectors of the transition matrix. In this case, the ratio of the probabilities of two adjacent states can be read off directly from the transition matrix via

$$\frac{P(M_{i+1})}{P(M_i)} = \frac{T(M_i \to M_{i+1})}{T(M_{i+1} \to M_i)}, \tag{A9}$$

yielding the weight difference

$$\begin{aligned}\eta(M_{i+1}) - \eta(M_i) &= -\ln\left(\frac{P(M_{i+1})}{P(M_i)}\right) \\ &= -\ln\left(\frac{T(M_i \to M_{i+1})}{T(M_{i+1} \to M_i)}\right).\end{aligned} \tag{A10}$$

Of course, when running the simulation, the system is still free to perform transitions between any values of M. However, these transitions are not registered in the transition matrix and thus are also not taken into account when calculating the weights. In the present study this was found to produce accurate and useful weight functions as transitions between distant values of M were rare and the entries in the second

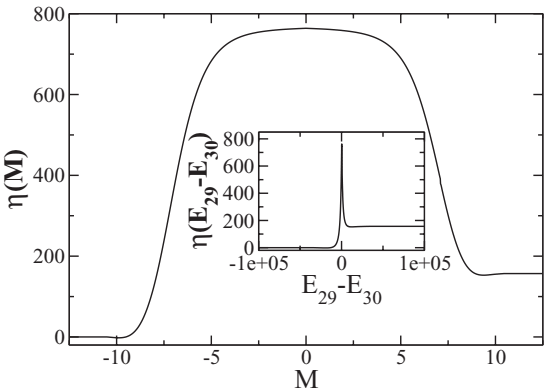

FIG. 13. Weight functions for the two-dimensional colloidal crystal with $N = 3240$ particles and structured walls at a misfit of $\Delta = 1.7$. The left minimum corresponds to states where the system was simulating the phase with 29 rows, the right minimum corresponds to 30 rows. Note that the weights have an exponential influence on the acceptance criterion. The large figure shows the weights plotted against the order parameter M as defined in Eq. (A2), the inset shows the same weight function plotted against the energy difference between the two phases in order to illustrate how the definition of the order parameter in the logarithm of the energy difference stretches the part around $M = 0$, where phase switches are most likely to happen.

off-diagonal elements of the transition matrix were already considerably smaller than the ones we used for the calculation of the weights.

By accumulating the transition matrix in the course of a simulation, one obtains an estimate for $P(M)$ which can be used to update $\eta(M)$, thereby allowing the simulation to explore a wide range of M. Repeated updates of $\eta(M)$ thus extend systematically the range of M over which one accumulates statistics for the weight function, until ultimately one reaches the gateway states. However, since updating the weight function during a simulation violates detailed balance, we chose to do this at rather infrequent intervals of 20 000 sweeps. Once the weight function extends to the gateway states, we stop updating the transition matrix and perform a long phase switch simulation with a fixed weight function in order to accumulate equilibrium free energy data.

An example of a weight function created for the system with $N = 3240$ particles (plus 432 fixed wall particles) at a misfit of $\Delta = 1.7$ is given in Fig. 13, also illustrating how the definition of the energy order parameter M given in Eq. (A2), which includes a logarithm of the energy difference, leads to a finer binning in the part closer to $M = 0$, where the phase switches are most likely to happen. In fact, to ensure that the transition matrix estimate of the weight function was sufficiently smooth and reliable in this region we reduced the number of bins in this region somewhat.

[1] G. Decker and J. B. Schlenoff (editors) *Multilayer Thin Films: Sequential Assembly of Nanocomposite Materials* (Wiley-VCH, Weinheim, 2002).

[2] E. L. Wolf, *Nanophysics ad Nanotechnology* (Wiley-VCH, Weinheim, 2002).

[3] Y. Champion and H. J. Fecht (editors) *Nano-architectured and Nano-structured Materials* (Wiley-VCH, Weinheim, 2004).

[4] C. N. R. Rao, A. Müller, and A. K. Cheetham (editors) *The Chemistry of Nanomaterials* (Wiley-VCH, Weinheim, 2004).

[5] R. Kelsall, I. W. Hamley, and M. Geoghegan (editors) *Nanoscale Science and Technology* (Wiley-VCH, Weinheim, 2005).

[6] D. Frenkel and B. Smit, *Understanding Molecular Simulations: From Algorithms to Applications* (Academic Press, San Diego, 2002).

[7] D. P. Landau and K. Binder, *A Guide to Monte Carlo Simulations in Statistical Physics*, 3rd ed. (Cambridge University Press, Cambridge, 2009).

[8] C. Chipot and A. Pohorille (editors) *Free Energy Calculations. Theory and Applications in Chemistry and Biology* (Springer, Berlin, 2007).

[9] A. D. Bruce and N. B. Wilding, Adv. Chem. Phys. **127**, 1 (2003).

[10] N. B. Wilding, in *Computer Simulations in Condensed Matter: From Materials to Chemical Biology*, edited by M. Ferrario, G. Ciccotti, and K. Binder (Springer, Berlin, 2006), Vol. 1, p. 39.

[11] M. Müller and J. J. de Pablo, in *Computer Simulations in Condensed Matter: From Materials to Chemical Biology*, edited by M. Ferrario, G. Ciccotti, and K. Binder (Springer, Berlin, 2006), Vol. 1, p. 67.

[12] J. G. Kirkwood, J. Chem. Phys. **3**, 300 (1935).

[13] K. Binder, Z. Phys. B **45**, 61 (1981).

[14] D. Frenkel and A. J. C. Ladd, J. Chem. Phys. **81**, 3188 (1984).

[15] T. Schilling and F. Schmid, J. Chem. Phys. **131**, 231102 (2009).

[16] F. Schmid and T. Schilling, Phys. Procedia **4**, 131 (2010).

[17] A. D. Bruce, N. B. Wilding, and G. J. Ackland, Phys. Rev. Lett. **79**, 3002 (1997).

[18] N. B. Wilding and A. D. Bruce, Phys. Rev. Lett. **85**, 5138 (2000).

[19] A. D. Bruce, A. N. Jackson, G. J. Ackland, and N. B. Wilding, Phys. Rev. E **61**, 906 (2000).

[20] A. N. Jackson, A. D. Bruce, and G. J. Ackland, Phys. Rev. E **65**, 036710 (2002).

[21] J. R. Errington, J. Chem. Phys. **120**, 3130 (2004).

[22] G. C. McNeil-Watson and N. B. Wilding, J. Chem. Phys. **124**, 064504 (2006).

[23] N. B. Wilding, J. Chem. Phys. **130**, 104103 (2009).

[24] A. Ricci, P. Nielaba, S. Sengupta, and K. Binder, Phys. Rev. E **75**, 011405 (2007).

[25] Y.-H. Chui, S. Sengupta, and K. Binder, Europhys. Lett. **83**, 58004 (2008).

[26] Y.-H. Chui, S. Sengupta, I. K. Snook, and K. Binder, J. Chem. Phys. **132**, 074701 (2010).

[27] Y.-H. Chui, S. Sengupta, I. K. Snook, and K. Binder, Phys. Rev. E **81**, 020403(R) (2010).

[28] K. Binder, Y.-H. Chui, P. Nielaba, A. Ricci, and S. Sengupta, in *Nanophenomena at Surfaces: Fundamentals of Exotic Condensed Matter Properties*, edited by M. Michailov (Springer, Berlin, 2011), p. 1.

[29] K. Zahn, J. M. Mendez-Alcaraz, and G. Maret, Phys. Rev. Lett. **79**, 175 (1997).

[30] Q. H. Wei, C. Bechinger, D. Rudhardt, and P. Leiderer, Phys. Rev. Lett. **81**, 2606 (1998).

[31] K. Zahn, R. Lenke, and G. Maret, Phys. Rev. Lett. **82**, 2721 (1999).

[32] K. Zahn and G. Maret, Phys. Rev. Lett. **85**, 3656 (2000).

[33] C. Eisenmann, P. Keim, U. Gasser, and G. Maret, J. Phys.: Condens. Matter **16**, S4095 (2004).

[34] K. Zahn, A. Wille, G. Maret, S. Sengupta, and P. Nielaba, Phys. Rev. Lett. **90**, 155506 (2003).

[35] H. König, R. Hund, K. Zahn, and G. Maret, Eur. Phys. J. E **18**, 287 (2005).

[36] M. Koppl, P. Henseler, A. Erbe, P. Nielaba, and P. Leiderer, Phys. Rev. Lett. **97**, 208302 (2006).

[37] L. Assoud, F. Ebert, P. Keim, R. Messina, G. Maret, and H. Löwen, J. Phys.: Condens. Matter **21**, 464114 (2009).

[38] F. Ebert, P. Dillmann, G. Maret, and P. Keim, Rev. Sci. Instrum. **80**, 083902 (2009).

[39] F. Ebert, G. Maret, and P. Keim, Eur. Phys. J. E **29**, 311 (2009).

[40] P. Henseler, A. Erbe, M. Koppl, P. Leiderer, and P. Nielaba, Phys. Rev. E **81**, 041402 (2010).

[41] N. A. Clark, B. J. Ackerson, and A. J. Hurd, Phys. Rev. Lett. **50**, 1459 (1983).

[42] A. Chowdhury, B. J. Ackerson, and N. A. Clark, Phys. Rev. Lett. **55**, 833 (1985).

[43] C. Bechinger, Q. W. Wei, and P. Leiderer, J. Phys.: Condens. Matter **12**, A425 (2000).
[44] C. Bechinger, M. Brunner, and P. Leiderer, Phys. Rev. Lett. **86**, 930 (2001).
[45] Y. J. Lai and L. I, Phys. Rev. E **64**, 015601(R) (2001).
[46] L. W. Teng, P. S. Tu, and L. I, Phys. Rev. Lett. **90**, 245004 (2003).
[47] R. A. Segalman, A. Hexemer, and E. J. Kramer, Phys. Rev. Lett. **91**, 196101 (2003).
[48] N. Kokubo, R. Besseling, and P. H. Kes, Phys. Rev. B **69**, 064504 (2004).
[49] G. Piacente, I. V. Schweigert, J. J. Betouras, and F. M. Peeters, Phys. Rev. B **69**, 045324 (2004).
[50] D. Chaudhuri and S. Sengupta, Phys. Rev. Lett. **93**, 115702 (2004).
[51] R. Haghgooie and P. S. Doyle, Phys. Rev. E **70**, 061408 (2004).
[52] W. G. Hoover, M. Ross, K. W. Johnson, D. Henderso, J. A. Barker, and B. C. Brown, J. Chem. Phys. **52**, 4931 (1970).
[53] K. Bagchi, H. C. Andersen, and W. Swope, Phys. Rev. E **53**, 3794 (1996).
[54] D. R. Nelson, in *Phase Transitions and Critical Phenomena*, edited by C. Domb and J. L. Lebowitz (Academic, London, 1983), Vol. 7, p. 1.
[55] P. M. Chaikin and T. C. Lubensky, *Principles of Condensed Matter Physics* (Cambridge University Press, Cambridge, 1995).
[56] Note that in [25–28] the walls were oriented along the y rather than the x direction.
[57] J. Villain, in *Ordering in Strongly Fluctuating Condensed Matter Systems*, edited by T. Riste (Plenum, New York, 1980), p. 222.
[58] M. Braun and Y. S. Kivshar, *The Frenkel-Kontorova Model: Concepts, Methods, and Applications* (Springer, Berlin, 2004).
[59] R. J. Speedy, Mol. Phys. **80**, 1105 (1993).
[60] D. Deb, D. Wilms, A. Winkler, P. Virnau, and K. Binder, Int. J. Mod. Phys. C. (to be published).
[61] G. R. Smith and A. D. Bruce, J. Phys. A **28**, 6623 (1995).
[62] J. S. Wang, T. K. Tay, and R. H. Swendsen, Phys. Rev. Lett. **82**, 476 (1999).
[63] J. S. Wang and R. H. Swendsen, J. Stat. Phys. **106**, 245 (2002).
[64] F. Wang and D. P. Landau, Phys. Rev. Lett. **86**, 2050 (2001).
[65] P. Virnau and M. Muller, J. Chem. Phys. **120**, 10925 (2004).
[66] A. Milchev, V. Yamakov, and K. Binder, Phys. Chem. Chem. Phys. **1**, 2083 (1999).
[67] A. Milchev, V. Yamakov, and K. Binder, Europhys. Lett. **47**, 675 (1999).
[68] A. M. Skvortsov, L. I. Klushin, and F. A. M. Leermakers, Europhys. Lett. **58**, 292 (2002).
[69] L. I. Klushin, A. M. Skvortsov, and F. A. M. Leermakers, Phys. Rev. E **69**, 061101 (2004).
[70] A. M. Skvortsov, L. I. Klushin, and F. A. M. Leermakers, J. Chem. Phys. **126**, 024905 (2007).
[71] D. I. Dimitrov, L. I. Klushin, A. M. Skvortsov, A. Milchev, and K. Binder, Eur. Phys. J. E **29**, 9 (2009).
[72] L. I. Klushin and A. M. Skvortsov, J. Phys. A: Math. Theor. **44**, 473001 (2011).
[73] M. Kikuchi and K. Binder, Europhys. Lett. **21**, 427 (1993).
[74] D. G. Walton, G. J. Kellogg, A. M. Mayes, P. Lambooy, and T. P. Russell, Macromolecules **27**, 6225 (1994).
[75] P. Lambooy, T. P. Russell, G. J. Kellogg, A. M. Mayes, P. D. Gallagher, and S. K. Satija, Phys. Rev. Lett. **72**, 2899 (1994).
[76] K. Binder, Adv. Polym. Sci. **138**, 1 (1999).
[77] D. Ausserre, V. A. Raghunathan, and M. Maaloum, J. Phys. II (France) **3**, 1485 (1993).
[78] L. G. MacDowell, V. K. Shen, and J. R. Errington, J. Chem. Phys. **125**, 034705 (2006); L. G. MacDowell, P. Virnau, M. Muller, and K. Binder, *ibid.* **120**, 5293 (2004).
[79] B. A. Berg and T. Neuhaus, Phys. Rev. Lett. **68**, 9 (1992); B. A. Berg, Int. J. Mod. Phys. C **4**, 249 (1993).
[80] D. Deb, A. Winkler, P. Virnau, and K. Binder, J. Chem. Phys. **136**, 134710 (2012).